

A Continuous, Drift-Compensated Impedimetric Thermal Flow Sensor for *In Vivo* Applications

Trevor Hudson, Alex Baldwin, and Ellis Meng

Department of Biomedical Engineering, University of Southern California, USA

ABSTRACT

We report a liquid flow sensor developed for biomedical applications based on electrochemical impedance (EI) measurements across a constantly-biased heating element. Prior EI-based flow transduction methods were limited to periodic measurements; this novel sensing approach is amenable to real time flow monitoring and does not require curve analysis or cooling between measurements to extract EI response to flow. The use of isolated reference electrodes in the sensor layout reduces sensitivity to environmental drift in ionic concentration and temperature by over $5\times$. Our sensor achieved a 2σ resolution of $35\ \mu\text{m}/\text{sec}$ between $0\text{--}200\ \mu\text{m}/\text{sec}$ in a flexible, biocompatible form factor.

INTRODUCTION

Liquid flow sensing is important for various industrial and medical applications. Of the many flow sensing technologies that have been developed, thermal flow sensing remains popular for its ease of implementation, simple structure, and minimal electronics overhead. Thermal flow sensors include some combination of heater and temperature sensor and are commonly categorized as: hot-film or anemometric, calorimetric, or time-of-flight [1]. Traditional thermal flow sensors are typically thermoresistive, in which resistive metal or semiconducting elements are used for both heating and temperature sensing. Sensors are typically constructed from hard materials such as silicon and metals due to their ease of fabrication and familiarity, as well as the linear temperature coefficient of resistance (TCR) of metals over a wide temperature range. However, the use of such materials *in vivo* requires additional packaging to prevent liquid and salt intrusion, which can decrease sensitivity; corrosion and formation of spurious conductive paths may occur with packaging failure [2].

Alternatively, sensors constructed using soft, biocompatible materials show promise for successful long-term implanted use. Our group previously presented an electrochemical-impedance (EI) based temperature sensor using exposed platinum electrodes on a Parylene substrate [3]. This method uses a high frequency signal to bypass the electrical double-layer to measure fluid resistance, which possesses an order-of-magnitude higher TCR than common metal sensing materials (human cerebrospinal fluid: $-2\%/^{\circ}\text{C}$ vs platinum: $0.39\%/^{\circ}\text{C}$ [4], [5]). Using EI temperature sensors, we previously demonstrated time-of-flight and calorimetric thermal flow sensing which use thermal pulses to minimize the effect of drift on long-term measurements [6], [7]. While effective in measuring steady flow rates under laboratory conditions, these designs require long warm-up and cooldown periods to capture the measurement signal, resulting in a maximum demonstrated flow sensing rate of one measurement each 30 seconds. They also suffered from drift due to stochastic changes in solution conductivity. Older examples of EI nonthermal

flow sensors using alternate tracer techniques also exist [8]–[10], but showed poor sensing resolution.

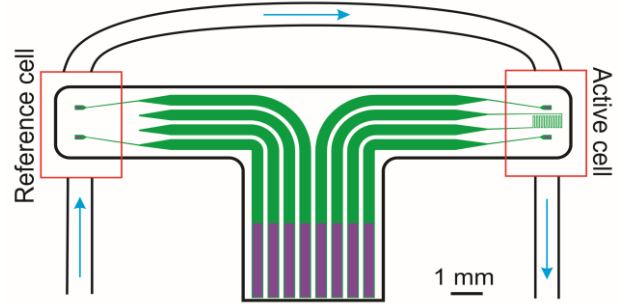


Figure 1: Schematic of device layout with two flow cells. The upstream cell contains reference electrodes only, while the downstream cell is actively heated. Each flow cell is enclosed by a thermoplastic module with luer connectors to facilitate integration. Flow cells are connected with a 3 cm length of silicone tubing, which isolates the reference cell from the heat signal.

Traditional thermal flow sensors often use an additional temperature sensing element as a reference. When fully isolated from the heater, the reference can be compared against the hot-film temperature signal to produce a differential signal, which eliminates common mode temperature fluctuations [11]. This strategy improves sensor response to any temperature drift which may occur. In this paper, we extend this concept by employing a reference EI cell to mitigate sensor drift from not only temperature variation, but also from changes in solution concentration and composition. We also introduce a novel sensing method in which the EI of fluid above a heated element is used to transduce flow rate in an impedimetric hot-film analog.

CONCEPT AND FABRICATION

The flow sensor consists of two EI-measurement cells in series. The reference cell is upstream and contains only a temperature sensor. The downstream active cell contains a heater and temperature sensor. As flow rate increases, more heat is removed by forced convection, resulting in a lower temperature. Both cells are fabricated as part of the same die and are connected by ~ 3 cm of silicone tubing.

When a potential is applied across two electrodes exposed to an ionic solution, current flows via movement of ions through solution; this relation is approximated by Ohm's law. The equivalent circuit is described by the solution resistance and two electrode-fluid interfaces and can be represented by the simplified Randles circuit. The equivalent impedance is:

$$Z_{eq} = R_S + \frac{2\omega C_{dl}}{R_{ct}\omega C_{dl} + 1} \quad (1)$$

where R_S is the solution resistance, R_{ct} is the electrode's charge transfer resistance, and C_{dl} is the double-layer capacitance.

The temperature coefficient of solution resistance for an ionic solution is high relative to typical sensing materials, which allows EI cells to be effective temperature detectors. This sensitivity, however, is impacted by the rate of change of the TCR with temperature. For example, the TCR of phosphate-buffered saline (PBS), a common analog for physiological fluid, decreases approximately 40% from 20 to 40°C [3]. Solution resistance is also a function of various other parameters such as solute concentration, solute identity (due to differences in electrical mobility), and presence of suspended solid particles [12]. The double-layer capacitance and charge transfer resistance are primarily determined by the surface area and material properties of the electrode, which are ideally stable, but can drift over time from degradative processes such as substrate layer delamination and biological deposition on electrode surfaces.

DC Power Supply

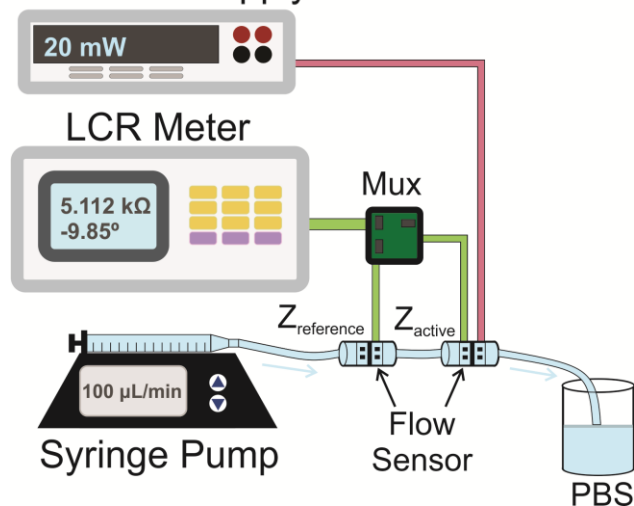


Figure 2: Phosphate-buffered saline (PBS) is pumped through the flow sensor to simulate physiological flows. Impedance is measured at 100 kHz using a LCR meter from both cells while the heater is biased with constant power.

To correct for these potential confounding factors, we acquire a differential impedance signal between the active and reference cells to eliminate common mode disturbances. The temperature sensors are separated into two cells to thermally isolate the reference sensor completely from the active heater, even at zero flow. Each cell is identical apart from the presence or absence of the resistive heater.

The fabrication process was previously described in [13]. First, 15 µm of Parylene C was deposited on a silicon carrier wafer. 2000 Å thick layer of Pt was then deposited via electron-beam evaporation and patterned by lift-off (AZ5214 photoresist). A second 15 µm Parylene insulating layer was deposited, after which electrodes (180×20 µm² area) and contact pads were exposed via a deep reactive ion etch in oxygen plasma using patterned AZ 4620 as an etch mask. Individual device dies were removed from the carrier and annealed under vacuum at 200°C for 48 hours to improve adhesion between Parylene layers. A thin polyetheretherketone spacer was added to support the contact pads and the assembly was inserted into a zero insertion force connector to establish external electrical

connections. Devices were packaged into a thermoplastic module (ID 3.25 mm). Silicone tubing (ID 1.58 mm) connected the reference and flow transduction cells.

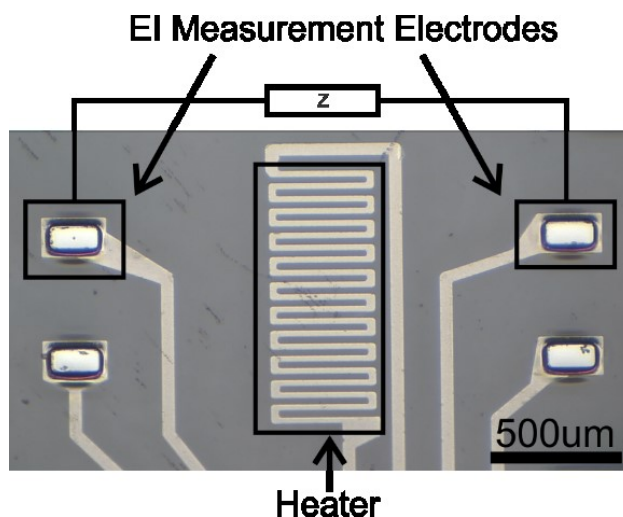


Figure 3: Microscope image of measurement cell. Central resistive trace acts as heater. Electrochemical impedance of fluid above heater is measured using exposed electrodes.

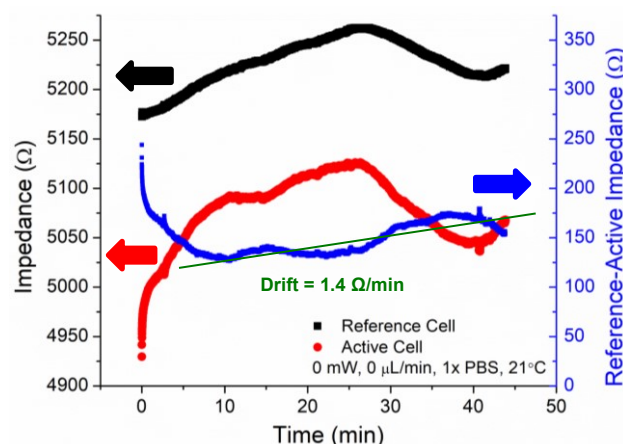


Figure 4: Two measurement cells in the same fluid path each detect the drift signal in environmental electrochemical impedance at zero flow, caused by stochastic changes.

EXPERIMENTAL METHOD

Flow sensing performance was characterized using 1× PBS flow set by a calibrated syringe pump connected to the sensor pair. Heating current to the active cell was supplied by a Keithley 2400 SourceMeter. A constant power of 20 mW (4°C overheat temperature) was delivered to the heater during flow transduction in order to dissipate constant heat flux into the fluid according to the Joule-Lenz law [14]; power regulation was achieved using proportional-integral-derivative feedback implemented in LabVIEW. Given that our flow sensor functions via temperature detection across the heater, constant temperature mode would not be expected to show any sensitivity to flow – this was confirmed experimentally (results not shown). Impedance across EI electrodes was measured using an Agilent E4980A precision LCR meter (100 kHz, 0.3 V_{P-P}). This signal was alternated between each device at 10 Hz using a multiplexer.

Flow rates were calibrated to the differential impedance signal between the active and reference cells. This signal was normalized to its initial value and to the reference impedance to minimize the effect of drift.

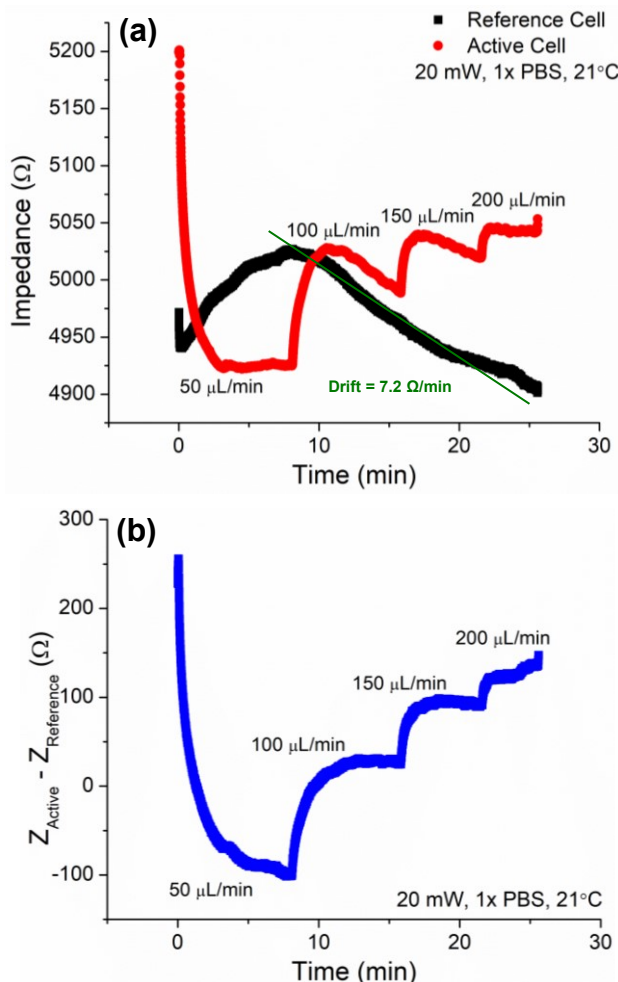


Figure 5: (a) Active cell impedance measurements alone cannot transduce flow rate due to environmental drift. (b) Monitoring the difference between the impedances of the reference and active electrodes resulted in sensitive tracking of flow rate.

RESULTS AND DISCUSSION

Prior to flow velocity measurement, it was necessary to demonstrate that adjacent reference and active measurement cells were able to detect congruent drift signals. In Figure 4, the impedance from each cell was measured with no flow or heater activation. These measurements in red and black were observed to be qualitatively similar over 45 minutes of measurement. The differential signal in blue varied only $\sim 50 \Omega$ after a 5 minute warmup period, resulting in a net drift of 1.4 Ω /minute.

Figure 5a shows impedance signals from each cell with the heater and pump active. The reference impedance signal in black shows a noticeable downward slope of $\sim 7.2 \Omega$ /min over the timespan of the experiment. This drift was not induced; we suspect it is the result of a temperature or concentration gradient occurring in our test setup. We exploit this drift as a basic model for drift that one might encounter during *in vivo* use. From the active signal in red,

we observed a similar negative drift. Clearly, the active cell alone is incapable of resolving flow rates due to this monotonic instability. Using the differential signal in blue, we observed more stable flow rate tracking (Figure 5b).

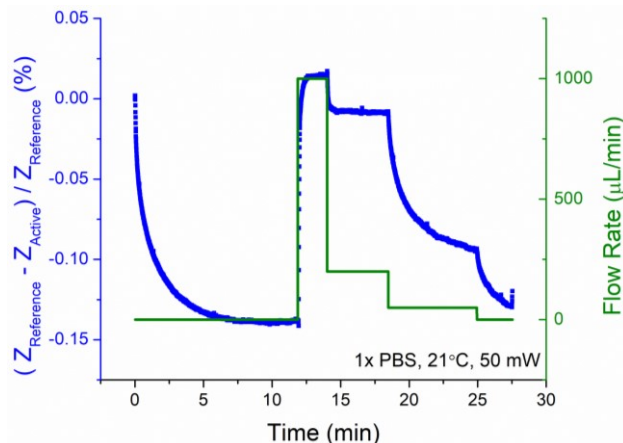


Figure 6: Comparing impedance between electrodes in two flow cells allows for flow rate transduction without waiting for a baseline measurement or cooling time between measurements.

Figure 6 shows the differential impedance acquired through the sensor and outputted flow rate simultaneously. A significant difference in sensitivity clearly was observed at different flow rates, as would be expected in a typical anemometer. For example, the difference in response between 1000 and 200 μ L/min was -0.023%, while the difference between 200 and 50 μ L/min was -0.103%, a 24-fold change in sensitivity. The sensor's time constant, defined as the time required for the sensor response to reach 63.2% of its final value, also varied significantly with flow rate and with initial sensor value – from 0 to 1000 μ L/min, the calculated time constant is 4.12 seconds, versus 60.93 seconds when changing from 50 to 100 μ L/min. These preliminary results will require further investigation.

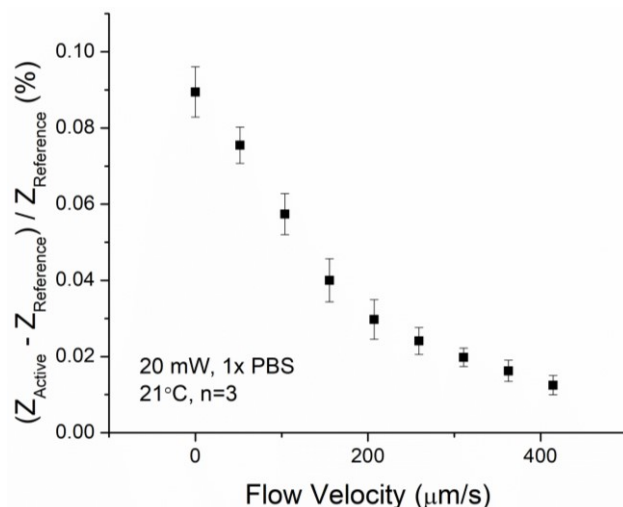


Figure 7: The normalized difference between reference and active impedance linearly transduces flow velocity at a 2σ resolution of 35 μ m/s up to 200 μ m/s.

Similarly, warm-up times for this sensor depend heavily on flow rate. At zero flow, the sensor requires 205.6 seconds to reach 10% of its final stable value. At 50

$\mu\text{L}/\text{min}$, this value is 170.0 seconds. The above warm-up times and time constants are longer than traditional thermal anemometers, which are typically in the millisecond range [15], and represent a weakness of this method. To more effectively use this flow sensor, we aim to improve these values by reducing the thermal inertia of the measurement system, which is a lumped value dependent upon specific heat, thermal conductivity, dimensions, and geometry of the system. Methods to decrease thermal inertia could include decreasing the inner diameter of the thermoplastic module, decreasing output power through the heater, or reducing the surface area of the heater. The thermal conductivity of our substrate material, Parylene C, is $0.084 \text{ W}/(\text{m}^*\text{K})$ at 298K, which compares favorably with silicon dioxide at $1.3 \text{ W}/(\text{m}^*\text{K})$ [16], [17], a common substrate in MEMS sensor fabrication. Thus, we suspect that minimal heat loss occurs through our substrate. This and other assumptions will be tested via finite element modeling in future publications.

Continuous flow transduction was tested over the range of 0-400 $\mu\text{m}/\text{sec}$ in Figure 7. A 2σ resolution of 35 $\mu\text{m}/\text{sec}$ was achieved within the linear range of 0-200 $\mu\text{m}/\text{sec}$, which was taken as the flow range. Using a more sophisticated calibration method would allow an extension of this range. Our sensor operates with a sensitivity of $-3.00\text{E}-4 \text{ } \%/(\mu\text{m}/\text{sec})$. We demonstrate a comparable resolution to other EI sensors in the literature while gaining the advantage of continuous sensing (Table 1).

Table 1: Comparing this work with other single-phase EI sensors [6, 8-10], we demonstrate comparable resolution as recent discrete sensors, while achieving continuous sensing.

Paper	Sensing Method	Resolution ($\mu\text{m}/\text{s}$)	Measurement Mode
Wu 2002	ToF, dissolved O_2 tracer	-	Discrete
Ayliffe 2003	Ionic pathway changes	4.60E5	Continuous
Yu 2015	ToF, microbubble tracer	896	Discrete
Baldwin 2018	Calorimetric	19.1	Discrete
This Work	"Hot-film" analog	35.3	Continuous

Previous versions of EI sensors used heat pulses to reduce the effect of drift on measurements. This requires heater timing control to implement, as well as some curve analysis of the resultant impedance vs time curve. In this paper, only arithmetic operations are required for sensor operation, which could reduce electronics complexity. Additionally, no cooldown period is required between flow measurements, which limited previous designs.

ACKNOWLEDGEMENTS

This work was funded in part under NSF EFRI-1332394 and by the Provost PhD Fellowship (TH). The

authors would like to thank Priya Lee for fabrication assistance, Dr. Kee Scholten for experimental input, and all the remaining members of the BML for help and support.

REFERENCES

- [1] J. T. W. Kuo, L. Yu, and E. Meng, "Micromachined Thermal Flow Sensors—A Review," *Micromachines*, vol. 3, no. 3, pp. 550–573, Jul. 2012.
- [2] J. W. Osenbach, "Corrosion-induced degradation of microelectronic devices," *Semicond. Sci. Technol.*, vol. 11, no. 2, 1995.
- [3] A. Baldwin, et al. "A Flexible, Microfabricated Impedimetric Temperature Sensor," presented at the Solid-State Sensors, Actuators and Microsystems Workshop, Hilton Head Island, South Carolina, 2018.
- [4] D. C. Giancoli, *Physics*, 4th ed. Prentice Hall, 1995.
- [5] S. B. Baumann et al., "The electrical conductivity of human cerebrospinal fluid at body temperature," *IEEE Trans. Biomed. Eng.*, vol. 44, no. 3, pp. 220–223, Mar. 1997.
- [6] A. Baldwin, L. Yu, and E. Meng, "An Electrochemical Impedance-Based Thermal Flow Sensor for Physiological Fluids," *J. Microelectromechanical Syst.*, vol. 25, no. 6, pp. 1015–1024, Dec. 2016.
- [7] A. Baldwin, T. Hudson, and E. Meng, "A calorimetric flow sensor for ultra-low flow applications using electrochemical impedance," in *2018 IEEE Micro Electro Mechanical Systems (MEMS)*, 2018, pp. 361–364.
- [8] L. Yu and E. Meng, "A dual mode microbubble pressure and flow sensor," in *2016 IEEE 29th International Conference on Micro Electro Mechanical Systems (MEMS)*, Shanghai, China, 2016, pp. 325–328.
- [9] H. E. Ayliffe and R. D. Rabbitt, "An electric impedance based microelectromechanical system flow sensor for ionic solutions," *Meas. Sci. Technol.*, vol. 14, no. 8, p. 1321, 2003.
- [10] J. Wu and W. Sansen, "Electrochemical time of flight flow sensor," *Sens. Actuators Phys.*, vol. 97–98, pp. 68–74, Apr. 2002.
- [11] M. Elwenspoek, "Thermal flow micro sensors," *IEEE TRANS MAGN*, 1999, vol. 2, pp. 423–435 vol.2.
- [12] L. Coury, "Conductance Measurements Part 1: Theory," *Curr. Sep.*, p. 6, 1999.
- [13] B. J. Kim and E. Meng, "Micromachining of Parylene C for bioMEMS," *Polym. Adv. Technol.*, vol. 27, no. 5, pp. 564–576, 2016.
- [14] D. J. Griffiths, *Introduction to Electrodynamics*, 4th ed. Cambridge University Press, 2017.
- [15] Sensirion, "LD20-2600B Liquid Flow Sensor." Feb 2018.
- [16] "Parylene Properties | Coating Types C, N & F" VSI Parylene, 2018.
- [17] A. Delan et al., "Thermal conductivity of ultra low-k dielectrics," *Microelectron. Eng.*, vol. 70, no. 2, pp. 280–284, Nov. 2003.

CONTACT

*E. Meng, tel: +1-213-740-6952; ellis.meng@usc.edu